

RESEARCH ARTICLE

A Population-Based Study of Four Genes Associated with Heroin Addiction in Han Chinese

Yunxiao Li¹, Xiaomeng Qiao¹, Fangyuan Yin¹, Hao Guo¹, Xin Huang¹, Jianghua Lai^{1,2}, Shuguang Wei^{1,2*}

1 College of Forensic Science, Xi'an Jiaotong University, Key Laboratory of Ministry of Public Health for Forensic Science, Xi'an, PR China, **2** Key Laboratory of Environment and Genes Related to Diseases, Xi'an Jiaotong University, Ministry of Education, Xi'an, PR China

* weisg@xjtu.edu.cn



OPEN ACCESS

Citation: Li Y, Qiao X, Yin F, Guo H, Huang X, Lai J, et al. (2016) A Population-Based Study of Four Genes Associated with Heroin Addiction in Han Chinese. PLoS ONE 11(9): e0163668. doi:10.1371/journal.pone.0163668

Editor: Yong-Gang Yao, Kunming Institute of Zoology, Chinese Academy of Sciences, CHINA

Received: June 2, 2016

Accepted: September 11, 2016

Published: September 27, 2016

Copyright: © 2016 Li et al. This is an open access article distributed under the terms of the [Creative Commons Attribution License](https://creativecommons.org/licenses/by/4.0/), which permits unrestricted use, distribution, and reproduction in any medium, provided the original author and source are credited.

Data Availability Statement: All relevant data are within the paper and its Supporting Information files.

Funding: This research was supported by the National Science Foundation of China (NSFC 81571856 and NSFC 81373247; <http://www.nsf.gov.cn>). NSFC 81571856 had roles in data collection and analysis, decision to publish. NSFC 81373247 had role in study design.

Competing Interests: The authors have declared that no competing interests exist.

Abstract

Recent studies have shown that variants in FAT atypical cadherin 3 (*FAT3*), kinectin 1 (*KTN1*), discs large homolog2 (*DLG2*) and deleted in colorectal cancer (*DCC*) genes influence the structure of the human mesolimbic reward system. We conducted a systematic analysis of the potential functional single nucleotide polymorphisms (SNPs) in these genes associated with heroin addiction. We scanned the functional regions of these genes and identified 20 SNPs for genotyping by using the SNaPshot method. A total of 1080 samples, comprising 523 cases and 557 controls, were analyzed. We observed that *DCC* rs16956878, rs12607853, and rs2292043 were associated with heroin addiction. The T alleles of rs16956878 ($p = 0.0004$) and rs12607853 ($p = 0.002$) were significantly enriched in the case group compared with the controls. A lower incidence of the C allele of rs2292043 ($p = 0.002$) was observed in the case group. In block 2 of *DCC* (rs2292043-rs12607853-rs16956878), the frequency of the T-T-T haplotype was significantly higher in the case group than in the control group ($p = 0.024$), and fewer C-C-C haplotypes ($p = 0.006$) were detected in the case group. *DCC* may be an important candidate gene in heroin addiction, and rs16956878, rs12607853, and rs2292043 may be risk factors, thereby providing a basis for further genetic and biological research.

Introduction

Heroin addiction is a chronic brain disease characterized by compulsive drug-seeking, drug abuse, physical dependence, tolerance, and relapse [1]. Heroin is one of the most commonly used drugs in China. At the end of 2014, a total of 2.955 million drug addicts were registered in China. Opioid drug addicts numbered 1.458 million, 49.3% of whom were heroin users. A total of 9.3 tons of heroin were seized in 2014. The direct economic losses resulting from drug addiction approach CNY 500 billion every year, representing a substantial economic burden to

individuals and families. Similarly to other neuropsychiatric diseases, drug addiction results from a combination of genetic and environmental factors [2]. Family, adoption, and twin studies have suggested that genetic factors account for 30–60% of the overall variance in the risk of developing drug addiction [3–5].

Recently, FAT atypical cadherin 3 (*FAT3*), kinectin 1 (*KTN1*), discs large homolog 2 (*DLG2*) and deleted in colorectal cancer (*DCC*) have been reported to be associated with the function of the human mesolimbic reward system [6], which is the neurobiological basis of drug addiction. Cadherin, encoded by the *FAT3* gene, regulates neuronal morphology by affecting cell interactions [7], a crucial mechanism of pathological memory formation during drug addiction [8, 9]. The *FAT3* gene affects the volume of the caudoputamen [6], which plays important roles in habit formation, motivation, and the mechanism of drug addiction [10]. *KTN1* is responsible for organelle transport and localization [11], and this protein is also closely associated with the formation and quantity of dendritic spines [12], which form the common anatomical substrate of drug addiction [9]. Another biological function of *KTN1* is facilitating vesicle binding with kinesin, this binding is followed by kinesin-driven vesicle fast anterograde transport in axons [13, 14], suggesting that *KTN1* is a promising candidate gene involved in drug addiction. Recently, the role of *DLG2* has been investigated in a multitude of neuropsychiatric diseases. Genetic variants in *DLG2* affect learning and cognitive flexibility [15]. Genetic mapping of habitual substance users has revealed that *DLG2* is over-expressed at the neural synapse [16]. The *DCC* gene encodes netrin-1 receptor, which affects axon guidance and migration [17]. *DCC* has been widely studied in a multitude of neuropsychiatric diseases. Sensitizing amphetamine pretreatment regimens result in selective upregulation of the expression of *DCC* in the ventral tegmental area of adult rodents [18], and *DCC* haploinsufficiency decreases sensitivity to the cocaine mediated enhancement of reward seeking behavior [19]. Furthermore, *DCC* is a regulator of maladaptive responses, such as tolerance, dependence and opioid-induced hyperalgesia to chronic morphine administration [20]. On the basis of these findings, these four genes may be important mediators of drug addiction. To the best of our knowledge, the roles of these genes in heroin addiction have not previously been reported.

Variations in gene functional regions may represent the most direct molecular mechanisms of disease [21]. The exon sequence can be transcribed into the final mRNA. Variations in exon regions may change the amino acid sequences. The most prominent example is brain-derived neurotrophic factor (*BDNF*), whose rs6265 SNP is directly associated with the clinical phenotype of drug addiction [22, 23]. Variations in promoter affect the efficiency of gene transcription. Variations in intron-exon borders may affect exon recognition and change the attributes of the alternative products [24, 25]. 5'UTRs are DNA regulatory sequences located in the 5' termini of protein-coding genes. These sequences can be transcribed to mRNA, but cannot be translated to protein. 5'UTRs contain a variety of regulatory elements, including the 5' cap, secondary structure, alternative 5'UTRs, internal ribosome entry sites, and upstream open reading frames (uORFs), among others. In general, 5'UTRs primarily regulate transcriptional initiation [26]. 3'UTRs are DNA regulatory sequences located downstream of the protein coding sequences, and these sequences primarily regulate gene expression at the post-transcriptional level, including transcriptional stability and cleavage, and polyadenylation, among others [27]. Because determining associations between functional polymorphisms and heroin addiction would be meaningful, we used HapMap (Han Chinese population) HCB data to systematically scan the promoter, 5'UTR, 3'UTR, exon, and intron-exon border regions of *FAT3*, *KTN1*, *DLG2* and *DCC*, and 20 SNPs were selected to do association analysis with heroin addiction.

Materials and Methods

Subjects

A total of 1080 individuals were recruited for the present study. All of these individuals were biologically unrelated individuals of China Han ancestry. Among them, 523 individuals were heroin addiction patients (mean age 45.13 ± 7.270 years) recruited from the Methadone Maintenance Treatment (MMT) Program at the Xi'an Mental Health Center between October 2013 and May 2015. At least two senior psychiatrists independently interviewed all patients, and urine testing and the Diagnostic and Statistical Manual of Mental Disorders, fourth revision (DSM-IVR) diagnostic criteria were applied to diagnose opioid addiction. A case vignette was generated to assist with the diagnosis, using a semi-structured interview with questions regarding (a) the age of onset and the duration of heroin use, (b) the quantity of the drug used during this period, (c) the route of administration (i.e., nasal inhalation or injection), (d) whether other substances were used or abused, and (e) comorbidity with any other psychiatric disorder. Participants meeting DSM-IVR criteria for an additional Axis I disorder; with a history of cigarette, alcohol, amphetamine, barbiturate, or benzodiazepine dependence; exhibiting mental illness or neurological diseases; or a history of hematological diseases, seizures, or other chronic physical illnesses were excluded.

The control cohort comprised 557 healthy people (mean age 45.80 ± 10.449 years) recruited from the health examination center at the First Hospital Affiliated with the Medical College of Xi'an Jiao Tong University. The selection criteria were: having no individual history of drug addiction or mental illness, and frequency matching to cases on the basis of gender and age.

All participants provided written informed consent. Our study protocol was approved by the Ethical Committee of Xi'an Mental Health Center, Xi'an, China and the methods were performed in accordance with the approved guidelines.

SNP selection

A total of 20 SNPs were selected on the basis of the following criteria: (1) location in functional region of the gene, including the promoter region, untranslated regions (UTRs), exons, and intron-exon borders, and (2) minor allele frequencies (MAF) greater than 0.05 on the basis of HapMap. The chromosomal positions of the six SNPs in *KTNI* (rs10146870, rs1138345, rs10483647, rs1951890, rs17128657, and rs945270) were searched from 55554095 to 55706484bp. The chromosomal positions of the six SNPs in *DCC* (rs17753970, rs934345, rs2229080, rs16956878, rs12607853, and rs2292043) were searched from 52338192 to 53536381bp. The chromosomal positions of the four SNPs in *FAT3* (rs10765565, rs4753069, rs2197678, and rs7927604) were searched from 92312328 to 92896960bp. The chromosomal positions of the four SNPs in *DLG2* (rs575050, rs2512676, rs17145219, and rs2507850) were searched from 83454513 to 85629270bp. The databases were HapMap and dbSNP (HCB), and the positions of these SNPs are listed in [Table 1](#).

Genotyping

Peripheral blood samples from the enrolled subjects were collected in EDTA-coated tubes. Genomic DNA was extracted from blood leukocytes by using E.Z.N.A.[™] Blood DNA Midi Kit (Omega Bio-Tek, Norcross, GA, USA) according to the manufacturer's instructions. A total of 20 SNPs were genotyped by using SNaPshot SNP technology. A segment of DNA surrounding each SNP (151–368 bp) was amplified in a 10- μ l PCR reaction containing 1X HotStarTaq buffer, 3.0 mM Mg²⁺, 0.3 mM dNTPs, 1 U of HotStarTaq polymerase (Qiagen Inc., USA), 1 μ l of DNA and 1 μ l of each PCR primer. The PCR program included an initial cycle at 95°C for

Table 1. Genotypic and allelic frequencies of gene polymorphisms in the control and case group and statistical results.

Gene	Variable	Position	MAF	Controls (557)		Cases (523)		P-value ^a	P-value ^b	P-value ^c	OR, 95% CI	
				No.	%	No.	%					
FAT3	rs10765565	Exon17	0.219					0.19	0.712	14.240		
	GG			345	61.9	321	61.4	0.849	16.980	0.976,0.764–1.248		
	GT			180	32.3	177	33.8	0.594	11.880	1.071,0.831–1.381		
	TT			32	5.7	25	4.8	0.478	9.560	0.824,0.481–1.410		
	G allele			870	78.1	819	78.3	0.910	18.200	1.012,0.825–1.241		
	T allele			244	21.9	227	21.7					
	rs4753069	Exon19	0.291					0.43	0.811	16.220		
	GG			284	51.0	269	51.4	0.883	17.660	1.018,0.802–1.293		
	GA			222	39.9	201	38.4	0.632	12.640	0.942,0.738–1.203		
	AA			51	9.2	53	10.1	0.586	11.720	1.119,0.747–1.676		
	G allele			790	70.9	739	70.7	0.892	17.840	0.987,0.820–1.189		
	A allele			324	29.1	307	29.3					
	rs2197678	3' UTR	0.289					0.178	0.432	8.640		
	CC			275	49.4	277	53.0	0.238	4.760	1.155,0.909–1.466		
	CT			242	43.4	207	39.6	0.197	3.940	0.853,0.669–1.087		
	TT			40	7.2	39	7.5	0.862	17.240	1.041,0.659–1.647		
	C allele			792	71.1	761	72.8	0.392	7.840	1.086,0.900–1.310		
	T allele			322	28.9	285	27.2					
	rs7927604	3' UTR	0.376					0.69	0.653	13.060		
	AA			219	39.3	201	38.4	0.765	15.300	0.963,0.754–1.231		
	AG			257	46.1	254	48.6	0.425	8.500	1.102,0.868–1.400		
	GG			81	14.5	68	13.0	0.463	9.260	0.878,0.621–1.243		
	A allele			695	62.4	656	62.7	0.875	17.500	1.014,0.852–1.207		
	G allele			419	37.6	390	37.3					
KTN1	rs10146870	5' near	0.403					0.33	0.562	11.240		
	GG			204	36.6	201	38.4	0.540	10.800	1.080,0.844–1.382		
	GC			257	46.1	244	46.7	0.866	17.320	1.021,0.804–1.297		
	CC			96	17.2	78	14.9	0.300	6.000	0.842,0.608–1.166		
	G allele			665	59.7	646	61.8	0.326	6.520	1.090,0.917–1.296		
	C allele			449	40.3	400	38.2					
		rs1138345	5' UTR	0.367					0.21	0.314	6.280	
		TT			230	41.3	229	43.8	0.407	8.140	1.107,0.870–1.410	
		GT			245	44.0	233	44.6	0.852	17.040	1.023,0.805–1.301	
		GG			82	14.7	61	11.7	0.138	2.760	0.765,0.536–1.091	
		T allele			705	63.3	691	66.1	0.178	3.560	1.129,0.946–1.347	
		G allele			409	36.7	355	33.9				
	rs10483647	Intron10	0.291					0.86	0.949	18.980		
	AA			281	50.4	269	51.4	0.746	14.920	1.040,0.819–1.321		
	AG			228	40.9	210	40.2	0.794	15.880	0.968,0.759–1.235		
	GG			48	8.6	44	8.4	0.904	18.080	0.974,0.635–1.494		
	A allele			790	70.9	748	71.5	0.760	15.200	1.029,0.854–1.240		
	G allele			324	29.1	298	28.5					
	rs1951890	Intron18	0.375					0.64	0.234	4.680		
	AA			220	39.5	218	41.7	0.465	9.300	1.095,0.859–1.396		
	AG			256	46.0	247	47.2	0.677	13.540	1.055,0.828–1.337		
	GG			81	14.5	58	11.1	0.090	1.800	0.733,0.511–1.051		

(Continued)

Table 1. (Continued)

Gene	Variable	Position	MAF	Controls (557)		Cases (523)		P-value ^a	P-value ^b	P-value ^c	OR, 95% CI
				No.	%	No.	%				
	A allele			696	62.5	683	65.3		0.173	3.460	1.130,0.948–1.347
	G allele			418	37.5	363	34.7				
	rs17128657	Intron20	0.338					0.028	0.061	1.220	
	AA			256	46.0	249	48.2		0.587	11.740	1.069,0.841–1.357
	AT			226	40.6	222	42.9		0.532	10.640	1.080,0.848–1.376
	TT			75	13.5	46	8.9		0.015	0.300	0.620,0.420–0.914
	A allele			738	66.2	720	69.6		0.093	1.860	1.168,0.974–1.401
	T allele			376	33.8	314	30.4				
	rs945270	3' near	0.190					0.96	0.018	0.360	
	GG			365	65.5	310	59.3		0.034	0.680	0.766,0.598–0.980
	GC			172	30.9	177	33.8		0.298	5.960	1.145,0.887–1.478
	CC			20	3.6	36	6.9		0.015	0.300	1.985,1.134–3.475
	G allele			902	81.0	797	76.2		0.007	0.140	0.752,0.612–0.925
	C allele			212	19.0	249	23.8				
<i>DLG2</i>	rs575050	5' near	0.409					0.45	0.750	15.000	
	TT			190	34.1	186	35.6		0.616	12.320	1.066,0.830–1.370
	TG			278	49.9	249	47.6		0.450	9.000	0.912,0.718–1.158
	GG			89	16.0	88	16.8		0.707	14.140	1.064,0.771–1.468
	T allele			658	59.1	621	59.4		0.886	17.720	1.013,0.853–1.202
	G allele			456	40.9	425	40.6				
	rs2512676	3' UTR	0.317					0.69	0.146	2.920	
	TT			262	47.0	260	49.7		0.379	7.580	1.113,0.877–1.413
	TG			237	42.5	226	43.2		0.826	16.520	1.027,0.807–1.308
	GG			58	10.4	37	7.1		0.053	1.060	0.655,0.426–1.008
	T allele			761	68.3	746	71.3		0.128	2.560	1.153,0.960–1.387
	G allele			353	31.7	300	28.7				
	rs17145219	3'UTR	0.230					0.39	0.066	1.320	
	CC			334	60.0	338	64.6		0.114	2.280	1.220,0.953–1.561
	CG			190	34.1	168	32.1		0.488	9.760	0.914,0.709–1.178
	GG			33	5.9	17	3.3		0.037	0.740	0.533,0.293–0.970
	C allele			858	77.0	844	80.7		0.037	0.740	1.247,1.013–1.534
	G allele			256	23.0	202	19.3				
	rs2507850	3' near	0.311					0.52	0.146	2.920	
	GG			268	48.1	261	49.9		0.557	11.140	1.074,0.846–1.364
	GA			232	41.7	226	43.2		0.604	12.080	1.066,0.837–1.357
	AA			57	10.2	36	6.9		0.050	1.000	0.648,0.419–1.002
	G allele			768	68.9	748	71.5		0.192	3.840	1.131,0.940–1.360
	A allele			346	31.1	298	28.5				
<i>DCC</i>	rs17753970	5' near	0.499					0.19	0.311	6.220	
	AA			132	23.7	145	27.7		0.130	2.600	1.235,0.940–1.624
	AG			294	52.8	259	49.5		0.284	5.680	0.878,0.691–1.114
	GG			131	23.5	119	22.8		0.766	15.320	0.958,0.722–1.271
	A allele			558	50.1	549	52.5		0.266	5.320	1.101,0.930–1.303
	G allele			556	49.9	497	47.5				
	rs934345	5' near	0.286					0.17	0.021	0.420	
	GG			277	49.7	304	58.1		0.006	0.120	1.403,1.103–1.784

(Continued)

Table 1. (Continued)

Gene	Variable	Position	MAF	Controls (557)		Cases (523)		P-value ^a	P-value ^b	P-value ^c	OR, 95% CI
				No.	%	No.	%				
	GC			241	43.3	187	35.8		0.012	0.240	0.730,0.571–0.932
	CC			39	7.0	32	6.1		0.558	11.160	0.866,0.534–1.404
	G allele			795	71.4	795	76.0		0.014	0.280	1.271,1.048–1.541
	C allele			319	28.6	251	24.0				
	rs2229080	Exon3	0.497					0.77	0.195	3.900	
	CC			139	25.0	125	23.9		0.687	13.740	0.944,0.715–1.247
	GC			282	50.6	245	46.8		0.214	4.280	0.859,0.677–1.091
	GG			136	24.4	153	29.3		0.073	1.460	1.280,0.977–1.677
	C allele			560	50.3	495	47.3		0.171	3.420	1.125,0.950–1.332
	G allele			554	49.7	551	52.7				
	rs16956878	3' UTR	0.443					0.24	0.0001	0.002	
	CC			180	32.3	112	21.5		0.0001	0.002	0.571,0.434–0.751
	TC			261	46.9	260	50.0		0.348	6.960	1.121,0.883–1.424
	TT			116	20.8	148	28.5		0.004	0.080	1.500,1.135–1.984
	C allele			621	55.7	484	46.5		0.00002	0.0004	1.447,1.221–1.715
	T allele			493	44.3	556	53.5				
	rs12607853	3' UTR	0.443					0.20	0.0003	0.006	
	CC			180	32.3	113	21.7		0.0001	0.002	0.577,0.439–0.759
	CT			260	46.7	267	51.3		0.151	3.020	1.191,0.938–1.513
	TT			117	21.0	140	26.9		0.026	0.520	1.375,1.038–1.821
	C allele			620	55.7	493	47.4		0.0001	0.002	1.393,1.175–1.650
	T allele			494	44.3	547	52.6				
	rs2292043	3' UTR	0.425					0.16	0.001	0.020	
	TT			192	34.5	223	42.9		0.006	0.120	1.413,1.105–1.807
	TC			256	46.0	235	45.2		0.735	14.700	0.959,0.755–1.219
	CC			109	19.6	62	11.9		0.001	0.020	0.553,0.394–0.775
	T allele			640	57.5	681	65.5		0.0001	0.002	1.405,1.180–1.673
	C allele			474	42.5	359	34.5				

P-value ^a for Hardy-Weinberg equilibrium in controls.

P-value ^b for genotype and allele frequency difference.

P-value ^c for P-value ^b adjusted by Bonferroni correction.

doi:10.1371/journal.pone.0163668.t001

2 min, 11 cycles at 94°C for 20 s, 65°C for 40 s, and 72°C for 90 s, 24 cycles at 94°C for 20 s, 59°C for 30 s, and 72°C for 90 s, with a final cycle at 72°C for 2 min, and an indefinite hold at 4°C. To purify the PCR products, 5 U of shrimp alkaline phosphatase (SAP) enzyme and 2 U of Exonuclease I (Exo I) were mixed with 10 µl of the PCR product, incubated for 1 hour at 37°C and inactivated for 15 min at 75°C. The purified PCR products were used in a SNaPshot multiple single-base extension reaction. The extension reaction system (10 µl) contained 5 µl of the SNaPshot Multiplex Ready Reaction Mix (Applied Biosystems Co Ltd., CA, USA), 2 µl of the purified PCR product, 1 µl of the extension reaction primers, and 2 µl of ultrapure water. The PCR program initiated at 96°C for 1 min, and this was followed by 28 cycles of 96°C for 10 s, 55°C for 5 s, and 60°C for 30 s, and an indefinite hold 4°C. The products were purified after incubation with 1 U of SAP for 1 hour at 37°C, and this was followed by inactivation for 15 minutes at 75°C. Subsequently, 0.5 µl of the purified product was added to 0.5 µl of 120 Liz SIZE STANDARD (Applied Biosystems, Foster City, CA, USA) and 9 µl of Hi-Di (Applied

Biosystems, Foster City, CA, USA), and this was followed by sequencing on an ABI3130XL Sequencer (Applied Biosystems, Foster City, CA, USA) after degeneration at 95°C for 5 minutes. The primary data were analyzed using GeneMapper 4.1 (Applied Biosystems Co., Ltd., USA). The genotypes were determined on the basis of the nucleotide present at the SNP site, visualized as either one or two color peaks.

For quality control, 5% of the subjects (54 subjects) were randomly selected and blinded researchers conducted genotyping again, with a reproducibility of 100%.

Expression quantitative trait locus analysis

The mRNA expression level and genotype data for significant SNPs were received from the SNPexp database (<http://tinyurl.com/snpexp>) [28]. The HapMap version for the genotype was HapMap2r23 unfiltered 3.96 million SNPs. The data from RNA expression levels were obtained from transcripts of lymphoblastoid cell lines from the same 45 unrelated Han Chinese individuals in Beijing. The correlations between the genotype and mRNA expression levels of significant SNPs were calculated by using linear regression and the Wald test.

Statistical analysis

The genotype and allele frequencies of each individual polymorphism and the Hardy-Weinberg equilibrium (HWE) of the control and case groups were calculated by using the chi-square test. The associations between polymorphisms or other categorical variables with heroin addiction were assessed by using Pearson's Chi-square test. Continuous variables, such as the dose of heroin used and the age of heroin addiction onset, were analyzed using a correlate test. *P* values were calculated on the basis of the codominance or dominance of the rare allele, or the heterosis and recessive models of rare allele inheritance.

We computed pairwise LD statistics (D' and r^2) and haplotype frequencies using Haploview 4.0 (Broad Institute of MIT and Harvard, Cambridge, MA). We constructed haplotype blocks based on the criteria of Gabriel et al [29]. When the frequency of the haplotype was less than 5%, this value was excluded from the statistic analysis. We used PHASE 2.1.1 [30] software to verify the composition and frequency of positive haplotypes and to conduct permutation tests.

We analyzed the gene-gene interaction using Multifactor Dimensionality Reduction (<http://sourceforge.net/projects/mdr/>) which identifies high dimensional gene-gene interactions [31].

P values are presented as two-sided, and $p < 0.05$ was considered statistically significant. We used Bonferroni's correction to adjust the test level, and the *p* value was multiplied by all 20 loci or the haplotypes of each gene. All statistical analyses were conducted using SPSS 20.0 software (SPSS Inc., Chicago, IL, USA).

Power analysis

A sufficient sample size was required in this genetics study [32]. Thus, we conducted a power analysis using a Power and Sample Size Program (<http://biostat.mc.vanderbilt.edu/wiki/Main/PowerSampleSize>).

Results

No significant deviation from HWE was observed for any of the SNPs in the case group. In the control group, the rs17128657 SNP statistically deviated from HWE ($p = 0.028$). Five blocks were identified in the linkage disequilibrium (LD) analysis of the case and control data. For the *KTN1* gene, block 1 contained five SNPs (rs17128657, rs1951890, rs10483647, rs1138345 and rs10146870). For the *DLG2* gene, block 1 contained three SNPs (rs2507850, rs2512676 and

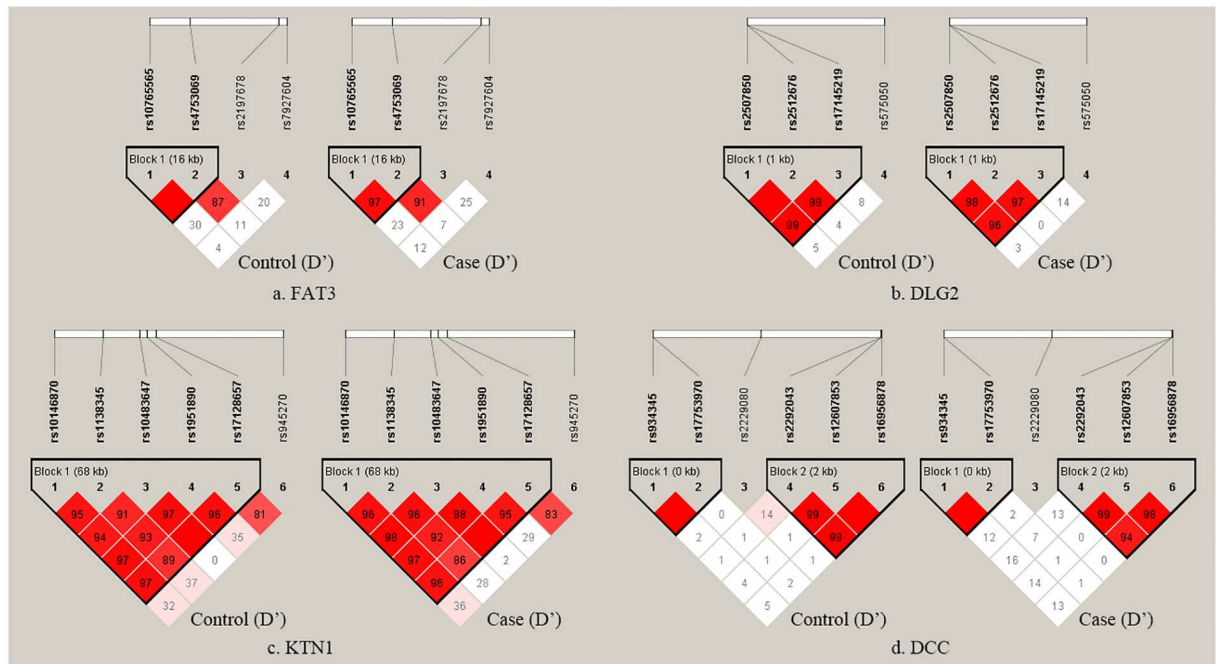


Fig 1. LD plot of the 20 SNPs in four genes in the control (left) and case (right) groups. (a) LD plot of the 4 SNPs of the *FAT3* gene in the control (left) and case (right) groups. (b) LD plot of the 4 SNPs of *DLG2* gene in the control (left) and case (right) groups. (c) LD plot of the 6 SNPs of the *KTN1* gene in the control (left) and case (right) groups. (d) LD plot of the 6 SNPs of the *DCC* gene in control (left) and case (right) groups. The values in squares are the D' calculated using pair-wise analyses. Empty squares indicate $D' = 1$ (i.e. complete LD between a pair of SNPs).

doi:10.1371/journal.pone.0163668.g001

rs17145219). For the *FAT3* gene, block 1 contained two SNPs (rs10765565 and rs4753069). For the *DCC* gene, block 1 contained two SNPs (rs934345 and rs17753970), and block 2 contained three SNPs (rs2292043, rs12607853 and rs16956878) (Fig 1). The distributions, frequencies and statistical analyses of the genotype, allele, and haplotype are provided in Tables 1 and 2.

For the *DCC* gene, the rs16956878 and rs12607853 genotypes were strongly associated with heroin addiction ($p = 0.002$, and $p = 0.006$, respectively). The T allele frequencies of rs16956878 ($p = 0.0004$, odds ratio [OR] = 1.447, 95% confidence interval [CI] = 1.221–1.715) and rs12607853 ($p = 0.002$, OR = 1.393, 95% CI = 1.175–1.650) were significantly higher in the case group than in the control subjects. A significant difference was also observed in the distribution of the genotype frequency for rs2292043 between the case and control groups ($p = 0.020$). Compared with the control group, the case group exhibited a lower frequency of the C allele ($p = 0.002$, OR = 1.405, 95% CI = 1.180–1.673). For the *KTN1* gene, addiction cases had a significantly higher frequency of the C allele than the control group at rs945270, but was not significant after Bonferroni correction ($p = 0.140$, OR = 0.752, 95% CI = 0.612–0.925). The sample size showed a 79%–91% power to detect associations with heroin addiction, with a presumed OR of 1.5, alpha value of 5%, and MAF ranging from 0.190 to 0.497.

In block 2 of *DCC* (rs2292043, rs12607853 and rs16956878), the frequency of the T-T-T haplotype was significantly higher than that in the control group ($p = 0.024$, OR = 1.381, 95% CI = 1.086–1.754), and fewer C-C-C haplotypes ($p = 0.006$, OR = 0.679, 95% CI = 0.530–0.870) were observed in the case group. The frequencies of these haplotypes in block 2 were similar to those obtained using PHASE (S1 Table). The p value was adjusted by using the 1000 permutations test ($p = 0.026$). On the basis of the results, we selected *DCC* rs16956878 as a representative of rs2292043, rs12607853 and rs16956878 for subsequent analyses.

Table 2. The frequencies of haplotypes in the four genes and their associations with the risk of heroin addiction.

Gene	Block	Haplotype	Controls(557)		Cases(523)		P-value ^a	P-value ^b	OR, 95% CI			
			No.	%	No.	%						
KTN1	block1	G-T-A-A-A	171	30.7	169	32.3	0.568	1.704	1.078,0.833–1.393			
			386	69.3	354	67.7						
		C-G-A-G-T	169	30.3	139	26.6				0.171	0.513	0.831,0.638–1.083
			388	69.7	384	73.4						
DLG2	block1	G-T-C	155	27.8	147	28.1	0.368	1.104	1.126,0.869–1.460			
			402	72.2	376	71.9						
		A-G-G	127	22.8	98	18.7				0.100	0.300	0.781,0.581–1.049
			430	77.2	425	81.3						
FAT3	block1	G-G	46	8.3	49	9.4	0.967	2.901	1.005,0.792–1.276			
			511	91.7	474	90.6						
		G-A	162	29.1	153	29.3				0.951	2.853	1.008,0.775–1.311
			395	70.9	370	70.8						
DCC	block1	T-G	122	21.9	112	21.4	0.846	2.538	0.972,0.727–1.298			
			435	78.1	411	78.6						
		G-A	279	50.1	275	52.6				0.413	1.239	1.105,0.870–1.403
			278	49.9	248	47.4						
DCC	block2	C-G	159	28.6	126	24.1	0.097	0.291	0.794,0.605–1.043			
			398	71.5	397	75.9						
		G-G	119	21.4	123	23.5				0.396	1.188	1.132,0.850–1.507
			438	78.6	400	76.5						
DCC	block2	T-T-T	246	44.2	273	52.2	0.008	0.024	1.381,1.086–1.754			
			311	55.8	250	47.8						
		C-C-C	237	42.6	175	33.5				0.002	0.006	0.679,0.530–0.870
			320	57.5	348	66.5						
DCC	block2	T-C-C	74	13.3	67	12.8	0.817	2.451	0.959,0.673–1.367			
			483	86.7	456	87.2						

P-value^a based on comparison of frequency distribution of all haplotypes for the combination of SNPs

P-value^b for P-value^a adjusted by Bonferroni correction.

doi:10.1371/journal.pone.0163668.t002

We analyzed the mRNA expression level and genotype data for *DCC* rs16956878. The mRNA expression levels of subjects with TT and CC genotypes were similar, and showed no significant differences (S2 Table).

The demographic and addiction characteristics were analyzed with respect to *DCC* rs16956878 (Table 3). Compared with the CC genotype, the TT and TC genotypes were more likely to be associated with more varied routes of heroin administration. The TT and TC genotypes, compared with the CC genotype, were more likely to be associated with heroin use through sniffing, smoking, intravenous injection, or compound delivery methods.

The results of the gene-gene interaction using MDR are listed in Table 4. The testing balance accuracy and cross validation consistency were the highest in models of rs12607853, rs2229080, and rs934345 (S1 Fig). Because it had the highest cross validation consistency and testing balance accuracy, the three-locus model was considered to be the optimal model.

Table 3. Demographic and addiction characteristics of DCC SNP rs16956878.

Variable	DCC rs16956878		
	CC	TC	TT
Age (year)	46.7±6.19	46.1±5.77	45.7±5.84
Gender (%)			
Male	21.3	49.8	28.9
Female	33.3	47.6	19.1
Occupation (%)			
Employed	19.2	54.1	26.7
Unemployed	23.1	47.4	29.5
Marital status (%)			
Unmarried	19.8	51.9	28.3
Married	23.0	48.0	29.0
Divorced or widowed	16.7	56.3	27.1
Route of heroin administration (%) ^a			
Sniffed or smoked	17.4	57.1	25.5
Injection via vein	21.9	51.7	26.5
Injection via muscle	36.4	36.4	27.3
Compound	26.5	27.9	45.6
Per-usage (gram)	0.3±0.14	0.3±0.34	0.3±0.18
Onset age (year)	29.1±6.68	29.4±6.41	28.6±6.73

^a Associated with route of heroin administration of rs16956878, $p = 0.003$.
The number that follows the ± sign is a standard deviation (s.d.).

doi:10.1371/journal.pone.0163668.t003

Discussion

Addiction is a disease resulting from interactions between genes and the environment [33]. The genetic susceptibility of heroin addiction primarily refers to the likelihood of individuals to use or become addicted to heroin because of differences in genetic factors [34–36]. Family, adoption, and twin studies have suggested that genetic factors account for 30–60% of the overall variance in the risk of developing drug addiction [3, 4]. The aim of our research was to identify additional genetic markers of heroin addiction through a case-control study. In addition to genetics, the substances effect is also an important factor leading to heroin addiction [37]. Indeed, the effect is different among the same people receiving different doses of heroin in a certain range [38]. However, not all people exposed to heroin will become addicted to this drug [37]. Our heroin addicts were recruited from the MMT Program and were diagnosed with heroin addiction. Our healthy controls were never self-exposed to heroin. Thus, our results should indicate that some subjects are more likely to become addicted to heroin, despite the effects of environmental factors.

Table 4. The results of gene-gene interactions using MDR.

Model	Training Bal. Acc	Testing Bal. Acc	CV Consistency
rs16956878	0.5545	0.5526	8/10
rs16956878 rs934345	0.5802	0.5499	6/10
rs12607853 rs2229080 rs934345	0.6141	0.5824	10/10
rs12607853 rs2229080 rs2512676 rs934345	0.6618	0.5721	7/10

doi:10.1371/journal.pone.0163668.t004

DCC is involved in axon guidance pathways, and its genetic variants influence the structure of the human mesolimbic reward system [6], which plays a key role in drug addiction. Our study provides direct evidence that polymorphisms of the *DCC* gene are associated with heroin addiction in the Chinese Han population.

In the present study, we observed that the T alleles of the *DCC* SNPs rs16956878 and rs12607853 were strongly associated with an increased risk of heroin addiction, whereas the C allele of *DCC* rs2292043 was associated with a decreased risk of heroin addiction, and these variants are located within the *DCC* 3' UTR. Moreover, we observed a significant increase in the T-T-T haplotype (rs2292043- rs12607853- rs16956878) in heroin addicts compared with the members of the control group. These results suggest that the subjects carrying the T-T-T haplotype are more likely to become addicted to heroin. The 3' UTR of a gene contains a number of regulatory sequences that are targets of a variety of regulatory molecules, including RNA binding proteins (RBPs) and small noncoding RNAs (ncRNAs), which recognize small cis-elements present in the 3' UTRs and determine the stability, cellular localization, and translation of the encoded mRNA [39, 40]. Among these regulatory molecules, microRNAs down-regulate genes and promote RNA cleavage through perfect base pairing with a target sequence [27]. By searching the MirSNP database [41], we observed that when rs12607853 allele changes from T to C, the mRNA of *DCC* can combine with hsa-miR-141-3p, and decrease *DCC* gene expression. When the rs2292043 allele changes from T to C, the mRNA of *DCC* can combine with hsa-miR-141-3689d, and decrease *DCC* gene expression. When the rs16956878 allele changes from T to C, the combined effect of the mRNA of *DCC* and hsa-miR-4666a-5p increases, thereby decreases *DCC* gene expression. Thus, in the heroin group, the higher frequency of T than C alleles, led to increased RNA expression. Our results are in agreement with the previous animal experimental conclusions. *DCC* haploinsufficiency mice showed blunted sensitivity to cocaine-mediated enhancement of reward seeking behavior [19]. We conducted an eQTL analysis of the mRNA expression level and examined the genotype data for *DCC* rs16956878 obtained from the SNPexp database. The mRNA expression levels of the subjects with TT and CC genotypes showed no significant differences. Because the RNA expression level and genotype data were obtained from only 45 unrelated individuals, the results may reflect the small sample size. Therefore, additional studies on the mRNA expression level of *DCC* and examination of the genotype data for rs16956878 with larger sample sizes are urgently needed. Grant et al. have reported an association between schizophrenia and the rs2270954 polymorphism in the 3' UTR of the *DCC* gene [42]. Peng et al have reported an association between schizophrenia and the rs2229080 polymorphism in the exon 3 of the *DCC* gene [43]. These results further support an important role for *DCC* in neuropsychiatric diseases. To confirm the link between the *DCC* gene and addiction, rs16956878 was analyzed, and the results suggested an association with the route of heroin administration. The rs16956878 TT and TC genotypes were associated with increased variance in the route of heroin administration and therefore might be associated with easier access to drugs. *DCC* is involved in axon guidance pathways and plays a critical functional role in the organization of brain development and in adult neuroplasticity [17, 44]. These results suggest that the *DCC* gene may contribute to the genetic basis of individual differences in susceptibility to heroin addiction.

KTN1 encodes the protein kinectin, which is primarily found in the endoplasmic reticulum in the dendrites and the soma of neurons [12]. *KTN1* plays a critical role in the regulation of neuronal cell shape, spreading, and migration through kinectin–kinesin interactions [45]. Disrupting the kinectin–kinesin interaction results in a morphological change to a rounded cell shape and reduced cell spreading and migration [45], which decreases the polarization of the neuronal architecture and the cellular complexity essential for neuronal functions [46]. Therefore, *KTN1* may affect the density or complexity of the dendritic spines in drug addicts, thereby

causing brain region-specific changes in the density of these structures[47]. The rs945270 SNP is located 50 kb downstream of the *KTN1* gene of 14q22.3. The C allele of rs945270 increases the expression of *KTN1* in the frontal cortex and putamen [48, 49]. In the present study, we identified a significantly higher C allele frequency in the heroin addiction group, although this result was not significant after correction. It has been suggested that subjects with the C allele in addicts might exhibit higher *KTN1* expression in the frontal cortex and putamen. Interestingly, amphetamine, cocaine and nicotine increase the spine density on the apical dendrites of the medial prefrontal cortex [50–52] and morphine significantly increases dendritic spine density in the orbital frontal cortex of adult rats[47]. Thus, *KTN1* may increase the density or complexity of dendritic spines in the frontal cortices of heroin addicts.

FAT3 is the human homolog of *Drosophila* FAT which inhibits Yokie through phosphorylation and subsequently activates the expanded-Hippo-Warts signaling cascade[53]. Phosphorylation of yes-associated protein 1(YAP1) in Hippo signaling inhibits the Wnt signaling cascade through interactions with β -catenin [54]. The cell polarity protein complex, Dlg/Lgl/Scrib affects the cell-cell contacts, thus leading to the deregulation of the actin cytoskeleton through interactions with Hippo pathways[55]. Netrin and Wnt signaling pathways play important roles in axon guidance[56]. Netrin signaling is primarily responsible for dorso-ventral (D/V)-graded distributions and Wnt signaling is primarily responsible for antero-posterior (A/P) distributions [57]. Kinesin-1 acts with DCC in sensory neuron position [58]. Thus, we speculated that these four genes might be involved in Hippo and/or Wnt signaling pathways. Studies have shown that the Wnt pathway regulates the susceptibility of chronic stress and addiction through the regulation of the differentiation of dopamine neurons in the mesolimbic reward system [59, 60]. Unfortunately, we did not obtain direct evidence from the KEGG pathway and PATHWAY STUDIO databases. The SNPs in the optimal model of gene-gene interaction were rs12607853, rs2229080, and rs934345, all of which are located in the *DCC* gene and no gene-gene interactions were detected. Thus, a pathway study of these genes would be meaningful in the future.

Conclusion

To the best of our knowledge, this is the first report demonstrating an association between heroin addiction and functional polymorphisms within the *DCC* gene in a homogeneous sampling population. However, further replication or validation across populations should be considered in the future. Moreover, studies of these polymorphisms and their expression are warranted to further the understanding of how these variants influence the expression and induction of these genes. These studies should help to elucidate the pathogenesis of heroin addiction and may offer a basis for the diagnosis and treatment of addiction.

Supporting Information

S1 Dataset. Genetic data in this study.

(XLSX)

S1 Fig. Optimal models determined by using MDR. Graphical model of rs12607853, rs2229080, and rs934345 (for SNP: 0 = no risk alleles, 1 = 1 risk allele, and 2 = 2 risk alleles). In each small square, the numbers represent the number of cases (left) and controls (right). Dark-shading for each square represents a high risk of disease, whereas light shading indicates a low risk of disease.

(TIF)

S1 Table. Haplotype frequencies estimated by using PHASE.

(DOCX)

S2 Table. DCC mRNA expression in the genotypes of rs16956878.
(DOCX)

Acknowledgments

We thank the patients and healthy volunteers for their participation in our study.

Author Contributions

Conceptualization: YL SW JL.

Data curation: YL XQ FY.

Formal analysis: YL XQ XH.

Funding acquisition: SW.

Methodology: YL XQ HG.

Resources: SW JL.

Software: HG XH.

Supervision: SW.

Validation: YL XQ FY HG XH JL SW.

Visualization: YL XQ.

Writing – original draft: YL SW.

Writing – review & editing: YL XQ FY HG XH JL SW.

References

1. Hosztafi S. [Heroin addiction]. *Acta pharmaceutica Hungarica*. 2011; 81(4):173–83. PMID: [22329304](#).
2. Vanyukov MM, Tarter RE. Genetic studies of substance abuse. *Drug and alcohol dependence*. 2000; 59(2):101–23. PMID: [10891624](#).
3. Kendler KS, Jacobson KC, Prescott CA, Neale MC. Specificity of genetic and environmental risk factors for use and abuse/dependence of cannabis, cocaine, hallucinogens, sedatives, stimulants, and opiates in male twins. *The American journal of psychiatry*. 2003; 160(4):687–95. doi: [10.1176/appi.ajp.160.4.687](#) PMID: [12668357](#).
4. Tsuang MT, Lyons MJ, Meyer JM, Doyle T, Eisen SA, Goldberg J, et al. Co-occurrence of abuse of different drugs in men: the role of drug-specific and shared vulnerabilities. *Archives of general psychiatry*. 1998; 55(11):967–72. PMID: [9819064](#).
5. van den Bree MB, Johnson EO, Neale MC, Pickens RW. Genetic and environmental influences on drug use and abuse/dependence in male and female twins. *Drug and alcohol dependence*. 1998; 52(3):231–41. PMID: [9839149](#).
6. Hibar DP, Stein JL, Renteria ME, Arias-Vasquez A, Desrivieres S, Jahanshad N, et al. Common genetic variants influence human subcortical brain structures. *Nature*. 2015; 520(7546):224–9. doi: [10.1038/nature14101](#) PMID: [25607358](#).
7. Deans MR, Krol A, Abraira VE, Copley CO, Tucker AF, Goodrich LV. Control of neuronal morphology by the atypical cadherin Fat3. *Neuron*. 2011; 71(5):820–32. doi: [10.1016/j.neuron.2011.06.026](#) PMID: [21903076](#).
8. Charness ME, Safran RM, Perides G. Ethanol inhibits neural cell-cell adhesion. *The Journal of biological chemistry*. 1994; 269(12):9304–9. PMID: [8132668](#).
9. Nestler EJ. Cellular basis of memory for addiction. *Dialogues in clinical neuroscience*. 2013; 15(4):431–43. PMID: [24459410](#).
10. Volkow ND, Morales M. The Brain on Drugs: From Reward to Addiction. *Cell*. 2015; 162(4):712–25. doi: [10.1016/j.cell.2015.07.046](#) PMID: [26276628](#).

11. Ong LL, Lim AP, Er CP, Kuznetsov SA, Yu H. Kinectin-kinesin binding domains and their effects on organelle motility. *The Journal of biological chemistry*. 2000; 275(42):32854–60. doi: [10.1074/jbc.M005650200](https://doi.org/10.1074/jbc.M005650200) PMID: [10913441](https://pubmed.ncbi.nlm.nih.gov/10913441/).
12. Toyoshima I, Sheetz MP. Kinectin distribution in chicken nervous system. *Neurosci Lett*. 1996; 211(3):171–4. PMID: [8817568](https://pubmed.ncbi.nlm.nih.gov/8817568/).
13. Ferreira A, Niclas J, Vale RD, Banker G, Kosik KS. Suppression of kinesin expression in cultured hippocampal neurons using antisense oligonucleotides. *The Journal of cell biology*. 1992; 117(3):595–606. PMID: [1533397](https://pubmed.ncbi.nlm.nih.gov/1533397/).
14. Elluru RG, Bloom GS, Brady ST. Fast axonal transport of kinesin in the rat visual system: functionality of kinesin heavy chain isoforms. *Molecular biology of the cell*. 1995; 6(1):21–40. PMID: [7538359](https://pubmed.ncbi.nlm.nih.gov/7538359/).
15. Nithianantharajah J, Komiyama NH, McKechnie A, Johnstone M, Blackwood DH, St Clair D, et al. Synaptic scaffold evolution generated components of vertebrate cognitive complexity. *Nat Neurosci*. 2013; 16(1):16–24. doi: [10.1038/nn.3276](https://doi.org/10.1038/nn.3276) PMID: [23201973](https://pubmed.ncbi.nlm.nih.gov/23201973/).
16. Nikpay M, Seda O, Tremblay J, Petrovich M, Gaudet D, Kotchen TA, et al. Genetic mapping of habitual substance use, obesity-related traits, responses to mental and physical stress, and heart rate and blood pressure measurements reveals shared genes that are overrepresented in the neural synapse. *Hypertension research: official journal of the Japanese Society of Hypertension*. 2012; 35(6):585–91. doi: [10.1038/hr.2011.233](https://doi.org/10.1038/hr.2011.233) PMID: [22297481](https://pubmed.ncbi.nlm.nih.gov/22297481/).
17. Hamasaki T, Goto S, Nishikawa S, Ushio Y. A role of netrin-1 in the formation of the subcortical structure striatum: repulsive action on the migration of late-born striatal neurons. *The Journal of neuroscience: the official journal of the Society for Neuroscience*. 2001; 21(12):4272–80. PMID: [11404412](https://pubmed.ncbi.nlm.nih.gov/11404412/).
18. Yetnikoff L, Eng C, Benning S, Flores C. Netrin-1 receptor in the ventral tegmental area is required for sensitization to amphetamine. *The European journal of neuroscience*. 2010; 31(7):1292–302. doi: [10.1111/j.1460-9568.2010.07163.x](https://doi.org/10.1111/j.1460-9568.2010.07163.x) PMID: [20345916](https://pubmed.ncbi.nlm.nih.gov/20345916/).
19. Reynolds LM, Gifuni AJ, McCrear ET, Shizgal P, Flores C. dcc haploinsufficiency results in blunted sensitivity to cocaine enhancement of reward seeking. *Behavioural brain research*. 2016; 298(Pt A):27–31. doi: [10.1016/j.bbr.2015.05.020](https://doi.org/10.1016/j.bbr.2015.05.020) PMID: [26005129](https://pubmed.ncbi.nlm.nih.gov/26005129/).
20. Liang DY, Zheng M, Sun Y, Sahbaie P, Low SA, Peltz G, et al. The Netrin-1 receptor DCC is a regulator of maladaptive responses to chronic morphine administration. *BMC genomics*. 2014; 15:345. doi: [10.1186/1471-2164-15-345](https://doi.org/10.1186/1471-2164-15-345) PMID: [24884839](https://pubmed.ncbi.nlm.nih.gov/24884839/).
21. Ramirez-Bello J, Vargas-Alarcon G, Tovilla-Zarate C, Fragoso JM. [Single nucleotide polymorphisms (SNPs): functional implications of regulatory-SNP (rSNP) and structural RNA (srSNPs) in complex diseases]. *Gaceta medica de Mexico*. 2013; 149(2):220–8. PMID: [23652189](https://pubmed.ncbi.nlm.nih.gov/23652189/).
22. Haerian BS. BDNF rs6265 polymorphism and drug addiction: a systematic review and meta-analysis. *Pharmacogenomics*. 2013; 14(16):2055–65. doi: [10.2217/pgs.13.217](https://doi.org/10.2217/pgs.13.217) PMID: [24279859](https://pubmed.ncbi.nlm.nih.gov/24279859/).
23. Su N, Zhang L, Fei F, Hu H, Wang K, Hui H, et al. The brain-derived neurotrophic factor is associated with alcohol dependence-related depression and antidepressant response. *Brain research*. 2011; 1415:119–26. doi: [10.1016/j.brainres.2011.08.005](https://doi.org/10.1016/j.brainres.2011.08.005) PMID: [21880305](https://pubmed.ncbi.nlm.nih.gov/21880305/).
24. Berget SM. Exon recognition in vertebrate splicing. *The Journal of biological chemistry*. 1995; 270(6):2411–4. PMID: [7852296](https://pubmed.ncbi.nlm.nih.gov/7852296/).
25. Rogers JH. The role of introns in evolution. *FEBS letters*. 1990; 268(2):339–43. PMID: [2200714](https://pubmed.ncbi.nlm.nih.gov/2200714/).
26. Pickering BM, Willis AE. The implications of structured 5' untranslated regions on translation and disease. *Seminars in cell & developmental biology*. 2005; 16(1):39–47. doi: [10.1016/j.semcdb.2004.11.006](https://doi.org/10.1016/j.semcdb.2004.11.006) PMID: [15659338](https://pubmed.ncbi.nlm.nih.gov/15659338/).
27. Yekta S, Shih IH, Bartel DP. MicroRNA-directed cleavage of HOXB8 mRNA. *Science (New York, NY)*. 2004; 304(5670):594–6. doi: [10.1126/science.1097434](https://doi.org/10.1126/science.1097434) PMID: [15105502](https://pubmed.ncbi.nlm.nih.gov/15105502/).
28. Holm K, Melum E, Franke A, Karlsen TH. SNPexp—A web tool for calculating and visualizing correlation between HapMap genotypes and gene expression levels. *BMC bioinformatics*. 2010; 11:600. doi: [10.1186/1471-2105-11-600](https://doi.org/10.1186/1471-2105-11-600) PMID: [21167019](https://pubmed.ncbi.nlm.nih.gov/21167019/).
29. Gabriel SB, Schaffner SF, Nguyen H, Moore JM, Roy J, Blumenstiel B, et al. The structure of haplotype blocks in the human genome. *Science (New York, NY)*. 2002; 296(5576):2225–9. doi: [10.1126/science.1069424](https://doi.org/10.1126/science.1069424) PMID: [12029063](https://pubmed.ncbi.nlm.nih.gov/12029063/).
30. Stephens M, Donnelly P. A comparison of bayesian methods for haplotype reconstruction from population genotype data. *American journal of human genetics*. 2003; 73(5):1162–9. doi: [10.1086/379378](https://doi.org/10.1086/379378) PMID: [14574645](https://pubmed.ncbi.nlm.nih.gov/14574645/).
31. Ritchie MD, Hahn LW, Moore JH. Power of multifactor dimensionality reduction for detecting gene-gene interactions in the presence of genotyping error, missing data, phenocopy, and genetic heterogeneity. *Genetic epidemiology*. 2003; 24(2):150–7. doi: [10.1002/gepi.10218](https://doi.org/10.1002/gepi.10218) PMID: [12548676](https://pubmed.ncbi.nlm.nih.gov/12548676/).

32. Liu C, Grennan KS. Current Practice of Genetics Research of Psychiatric Disorders. *Journal of Psychiatry and Brain Science*. 2016; 1(1):1.
33. Enoch MA. The influence of gene-environment interactions on the development of alcoholism and drug dependence. *Current psychiatry reports*. 2012; 14(2):150–8. doi: [10.1007/s11920-011-0252-9](https://doi.org/10.1007/s11920-011-0252-9) PMID: [22367454](https://pubmed.ncbi.nlm.nih.gov/22367454/).
34. Reed B, Butelman ER, Yuferov V, Randesi M, Kreek MJ. Genetics of opiate addiction. *Current psychiatry reports*. 2014; 16(11):504. doi: [10.1007/s11920-014-0504-6](https://doi.org/10.1007/s11920-014-0504-6) PMID: [25209027](https://pubmed.ncbi.nlm.nih.gov/25209027/).
35. Kreek MJ, Levran O, Reed B, Schlussman SD, Zhou Y, Butelman ER. Opiate addiction and cocaine addiction: underlying molecular neurobiology and genetics. *The Journal of clinical investigation*. 2012; 122(10):3387–93. doi: [10.1172/jci60390](https://doi.org/10.1172/jci60390) PMID: [23023708](https://pubmed.ncbi.nlm.nih.gov/23023708/).
36. Kreek MJ, Bart G, Lilly C, LaForge KS, Nielsen DA. Pharmacogenetics and human molecular genetics of opiate and cocaine addictions and their treatments. *Pharmacological reviews*. 2005; 57(1):1–26. doi: [10.1124/pr.57.1.1](https://doi.org/10.1124/pr.57.1.1) PMID: [15734726](https://pubmed.ncbi.nlm.nih.gov/15734726/).
37. Demaret I, Lemaitre A, Anseau M. [Heroin]. *Revue medicale de Liege*. 2013; 68(5–6):287–93. PMID: [23888578](https://pubmed.ncbi.nlm.nih.gov/23888578/).
38. Warner-Smith M, Darke S, Lynskey M, Hall W. Heroin overdose: causes and consequences. *Addiction (Abingdon, England)*. 2001; 96(8):1113–25. doi: [10.1080/09652140120060716](https://doi.org/10.1080/09652140120060716) PMID: [11487418](https://pubmed.ncbi.nlm.nih.gov/11487418/).
39. Xie X, Lu J, Kulbokas EJ, Golub TR, Mootha V, Lindblad-Toh K, et al. Systematic discovery of regulatory motifs in human promoters and 3' UTRs by comparison of several mammals. *Nature*. 2005; 434(7031):338–45. doi: [10.1038/nature03441](https://doi.org/10.1038/nature03441) PMID: [15735639](https://pubmed.ncbi.nlm.nih.gov/15735639/).
40. Chen JM, Ferec C, Cooper DN. A systematic analysis of disease-associated variants in the 3' regulatory regions of human protein-coding genes II: the importance of mRNA secondary structure in assessing the functionality of 3' UTR variants. *Human genetics*. 2006; 120(3):301–33. doi: [10.1007/s00439-006-0218-x](https://doi.org/10.1007/s00439-006-0218-x) PMID: [16807757](https://pubmed.ncbi.nlm.nih.gov/16807757/).
41. Liu C, Zhang F, Li T, Lu M, Wang L, Yue W, et al. MirSNP, a database of polymorphisms altering miRNA target sites, identifies miRNA-related SNPs in GWAS SNPs and eQTLs. *BMC genomics*. 2012; 13:661. doi: [10.1186/1471-2164-13-661](https://doi.org/10.1186/1471-2164-13-661) PMID: [23173617](https://pubmed.ncbi.nlm.nih.gov/23173617/).
42. Grant A, Fathalli F, Rouleau G, Joobor R, Flores C. Association between schizophrenia and genetic variation in DCC: a case-control study. *Schizophr Res*. 2012; 137(1–3):26–31. doi: [10.1016/j.schres.2012.02.023](https://doi.org/10.1016/j.schres.2012.02.023) PMID: [22418395](https://pubmed.ncbi.nlm.nih.gov/22418395/).
43. Yan P, Qiao X, Wu H, Yin F, Zhang J, Ji Y, et al. An Association Study Between Genetic Polymorphisms in Functional Regions of Five Genes and the Risk of Schizophrenia. *Journal of molecular neuroscience: MN*. 2016; 59(3):366–75. doi: [10.1007/s12031-016-0751-6](https://doi.org/10.1007/s12031-016-0751-6) PMID: [27055860](https://pubmed.ncbi.nlm.nih.gov/27055860/).
44. Flores C, Manitt C, Rodaros D, Thompson KM, Rajabi H, Luk KC, et al. Netrin receptor deficient mice exhibit functional reorganization of dopaminergic systems and do not sensitize to amphetamine. *Molecular psychiatry*. 2005; 10(6):606–12. doi: [10.1038/sj.mp.4001607](https://doi.org/10.1038/sj.mp.4001607) PMID: [15534618](https://pubmed.ncbi.nlm.nih.gov/15534618/).
45. Zhang X, Tee YH, Heng JK, Zhu Y, Hu X, Margadant F, et al. Kinectin-mediated endoplasmic reticulum dynamics supports focal adhesion growth in the cellular lamella. *Journal of cell science*. 2010; 123(Pt 22):3901–12. doi: [10.1242/jcs.069153](https://doi.org/10.1242/jcs.069153) PMID: [20980389](https://pubmed.ncbi.nlm.nih.gov/20980389/).
46. Setou M, Hayasaka T, Yao I. Axonal transport versus dendritic transport. *Journal of neurobiology*. 2004; 58(2):201–6. doi: [10.1002/neu.10324](https://doi.org/10.1002/neu.10324) PMID: [14704952](https://pubmed.ncbi.nlm.nih.gov/14704952/).
47. Robinson TE, Gorny G, Savage VR, Kolb B. Widespread but regionally specific effects of experimenter- versus self-administered morphine on dendritic spines in the nucleus accumbens, hippocampus, and neocortex of adult rats. *Synapse (New York, NY)*. 2002; 46(4):271–9. doi: [10.1002/syn.10146](https://doi.org/10.1002/syn.10146) PMID: [12373743](https://pubmed.ncbi.nlm.nih.gov/12373743/).
48. Hernandez DG, Nalls MA, Moore M, Chong S, Dillman A, Trabzuni D, et al. Integration of GWAS SNPs and tissue specific expression profiling reveal discrete eQTLs for human traits in blood and brain. *Neurobiology of disease*. 2012; 47(1):20–8. doi: [10.1016/j.nbd.2012.03.020](https://doi.org/10.1016/j.nbd.2012.03.020) PMID: [22433082](https://pubmed.ncbi.nlm.nih.gov/22433082/).
49. Ramasamy A, Trabzuni D, Guelfi S, Varghese V, Smith C, Walker R, et al. Genetic variability in the regulation of gene expression in ten regions of the human brain. *Nat Neurosci*. 2014; 17(10):1418–28. doi: [10.1038/nn.3801](https://doi.org/10.1038/nn.3801) PMID: [25174004](https://pubmed.ncbi.nlm.nih.gov/25174004/).
50. Crombag HS, Gorny G, Li Y, Kolb B, Robinson TE. Opposite effects of amphetamine self-administration experience on dendritic spines in the medial and orbital prefrontal cortex. *Cerebral cortex (New York, NY: 1991)*. 2005; 15(3):341–8. doi: [10.1093/cercor/bhh136](https://doi.org/10.1093/cercor/bhh136) PMID: [15269111](https://pubmed.ncbi.nlm.nih.gov/15269111/).
51. DePoy LM, Gourley SL. Synaptic Cytoskeletal Plasticity in the Prefrontal Cortex Following Psychostimulant Exposure. *Traffic (Copenhagen, Denmark)*. 2015; 16(9):919–40. doi: [10.1111/tra.12295](https://doi.org/10.1111/tra.12295) PMID: [25951902](https://pubmed.ncbi.nlm.nih.gov/25951902/).

52. Gonzalez CL, Gharbawie OA, Whishaw IQ, Kolb B. Nicotine stimulates dendritic arborization in motor cortex and improves concurrent motor skill but impairs subsequent motor learning. *Synapse* (New York, NY). 2005; 55(3):183–91. doi: [10.1002/syn.20106](https://doi.org/10.1002/syn.20106) PMID: [15635590](https://pubmed.ncbi.nlm.nih.gov/15635590/).
53. Katoh M. Function and cancer genomics of FAT family genes (review). *International journal of oncology*. 2012; 41(6):1913–8. doi: [10.3892/ijo.2012.1669](https://doi.org/10.3892/ijo.2012.1669) PMID: [23076869](https://pubmed.ncbi.nlm.nih.gov/23076869/).
54. Imajo M, Miyatake K, Imura A, Miyamoto A, Nishida E. A molecular mechanism that links Hippo signaling to the inhibition of Wnt/beta-catenin signalling. *The EMBO journal*. 2012; 31(5):1109–22. doi: [10.1038/emboj.2011.487](https://doi.org/10.1038/emboj.2011.487) PMID: [22234184](https://pubmed.ncbi.nlm.nih.gov/22234184/).
55. Enomoto M, Igaki T. Deciphering tumor-suppressor signaling in flies: genetic link between Scribble/Dlg/Lgl and the Hippo pathways. *Journal of genetics and genomics = Yi chuan xue bao*. 2011; 38(10):461–70. doi: [10.1016/j.jgg.2011.09.005](https://doi.org/10.1016/j.jgg.2011.09.005) PMID: [22035867](https://pubmed.ncbi.nlm.nih.gov/22035867/).
56. Tang X, Wadsworth WG. SAX-3 (Robo) and UNC-40 (DCC) regulate a directional bias for axon guidance in response to multiple extracellular cues. *PloS one*. 2014; 9(10):e110031. doi: [10.1371/journal.pone.0110031](https://doi.org/10.1371/journal.pone.0110031) PMID: [25333948](https://pubmed.ncbi.nlm.nih.gov/25333948/).
57. Levy-Strumpf N. Orchestrating A/P and D/V guidance—A Wnt/Netrin tale. *Worm*. 2016; 5(1): e1146857. doi: [10.1080/21624054.2016.1146857](https://doi.org/10.1080/21624054.2016.1146857) PMID: [27073738](https://pubmed.ncbi.nlm.nih.gov/27073738/).
58. Barsi-Rhyne BJ, Miller KM, Vargas CT, Thomas AB, Park J, Bremer M, et al. Kinesin-1 acts with netrin and DCC to maintain sensory neuron position in *Caenorhabditis elegans*. *Genetics*. 2013; 194(1):175–87. doi: [10.1534/genetics.113.149310](https://doi.org/10.1534/genetics.113.149310) PMID: [23475988](https://pubmed.ncbi.nlm.nih.gov/23475988/).
59. Wilkinson MB, Dias C, Magida J, Mazei-Robison M, Lobo M, Kennedy P, et al. A novel role of the WNT-dishevelled-GSK3beta signaling cascade in the mouse nucleus accumbens in a social defeat model of depression. *The Journal of neuroscience: the official journal of the Society for Neuroscience*. 2011; 31(25):9084–92. doi: [10.1523/jneurosci.0039-11.2011](https://doi.org/10.1523/jneurosci.0039-11.2011) PMID: [21697359](https://pubmed.ncbi.nlm.nih.gov/21697359/).
60. Luo SX, Huang EJ. Dopaminergic Neurons and Brain Reward Pathways: From Neurogenesis to Circuit Assembly. *The American journal of pathology*. 2016; 186(3):478–88. doi: [10.1016/j.ajpath.2015.09.023](https://doi.org/10.1016/j.ajpath.2015.09.023) PMID: [26724386](https://pubmed.ncbi.nlm.nih.gov/26724386/).